CHAPTER 106

NUMERICAL SIMULATION OF BEACH PROFILE CHANGES

Hitoshi Nishimura*
Tsuguo Sunamura**

ABSTRACT

This paper presents an overall numerical model for predicting beach profile changes due to waves. The local rate of net on/offshore sediment transport is empirically formulated as a function of the Ursell number and Hallermeier parameter. A sub-model of two-dimensional wave transformation includes the wave shoaling, breaking and damping in a surf zone. It is combined with another sub-model of beach profile change for the analyses of wave-profile interaction. The validity of the model is examined through hindcasting of profile changes observed in ordinary and prototype-scale flumes.

1. INTRODUCTION

In planning countermeasures against beach erosion, which is raising serious problems at many coast in the world, it is indispensable to understand the interaction between waves and beach profiles. This paper deals with a numerical model for the prediction of beach profile changes under given conditions of incident waves, bed material and initial profile. The process of profile change is simulated through repetitive calculation of two-dimensional wave transformation and net sediment transport due to waves. Similar trials were made also by Mizuguchi and Mori (1981) and Shibayama (1984).

For these years, trials have been made to establish a more advanced numerical model for analyzing three-dimensional beach processes. Nevertheless, studies on two-dimensional models such as beach profile models and shoreline models are meaningful particularly from the engineering point of view, since it seems to be impossible for the time being to apply a three-dimensional model to the analyses of long-term and/or wide-range beach transformations.

2. MODELING OF TWO-DIMENSIONAL WAVE TRANSFORMATION

Several methods are available for the numerical simulation of wave transformation in a shallow region. Among them, the simplest method based on the law of wave energy conservation will be most relevant here, since the calculation of local wave heights only is required in

* Associate Professor, Institute of Engineering Mechanics, University of Tsukuba, Sakura, Niihari, Ibaraki 305, Japan.
** Associate Professor, Institute of Geoscience, ditto.

modeling of this type. It is also to be borne in mind that the present model involves a net sediment transport rate formula, whose accuracy cannot be so high as yet.

For a steady field of uni-directional waves, the equation governing the variation of wave energy density is written as

$$\frac{\partial EC_g}{\partial x}+\Gamma=0 \tag{1}$$

where x is the shoreward coordinate, E is the wave energy density ($E=\rho gH^2/8$, ρ is the density of water, g is the gravitational acceleration and H is the wave height), C_g is the group velocity of waves, and Γ represents the wave damping mainly associated with breaking. Nishimura (1982) suggested that the wave height attenuation after breaking is well simulated, if the wave energy dissipation is assumed to be proportional to the energy density ($\Gamma=\alpha E$) with α regarded as a function of the water depth. Izumiya and Horikawa (1984) investigated the damping of waves more precisely to evaluate separately the effects of bottom friction and internal turbulence produced by breaking:

$$\Gamma=[\sqrt{2}(2n-1)C_f+C_t]\sqrt{\frac{2n-1}{\rho}\left(\frac{E}{d}\right)^3} \tag{2}$$

where n is the ratio of group velocity to phase velocity of waves, and d is the substantial water depth including wave setup.

The frictional coefficient C_f is normally assumed to take a value of the order 0.01. Another coefficient C_t , which represents the effect of turbulence in the surf zone, is given as

$$C_t=\beta_0\sqrt{nE/\rho gd^2-0.09} \tag{3}$$

where the value of β_0 is about 1.8, although it is affected by the bottom slope to a certain extent. The coefficient C_t is set to be zero before breaking or when $nE/\rho gd^2 < 0.09$. The breaking point is judged by use of the breaker indices given by Goda (1970).

For the numerical integration of Eq. (1), the variables are discretized and the equation is rewritten into a finite difference form. Computation points are uniformly distributed along the x-axis. Then, the wave energy (and, therefore, the wave height) at each point can be determined successively from the offshore to the shore, if the incident wave height and period are given.

Radiation stress accompanying monochromatic waves is easily evaluated from the energy density. Since the gradient of the stress balances with gravitational component of water surface slope,

$$\frac{\partial \zeta}{\partial x}+\frac{1}{\rho gd}\frac{\partial}{\partial x}\left[\left(2n-\frac{1}{2}\right)E\right]=0 \tag{4}$$

The surface elevation due to wave setup is given through the numerical integration of the above equation. In this case, Eqs. (1) and (4) have to be solved simultaneously, because the substantial water depth is the sum of ζ and the still water depth h . The amount of wave setup is actually very small except in a swash zone and it is sufficient to revise the values of ζ only when effective changes appears in d .

3. FORMULATION OF SEDIMENT TRANSPORT RATE

In order to measure a net sediment transport rate in a wave flume, a tray method (Sunamura,1982) was employed. A rectangular tray, the width of which is equal to that of the flume, is divided into two equivalent compartments by a thin metal splitter having the tray width. The compartments are filled with equal mass of sediment to be tested. The surface of sediment is manually smoothed and the splitter is removed. Then waves are allowed to act for a certain period of time. After completion of wave action, the splitter is returned to the original position. The sediment is separately taken out from each compartment and weighed after complete drying. From the difference in sediment mass, the direction and rate of net sediment transport are determined at a fair level of accuracy.

A wave flume 12 m long, 40 cm high, and 20 cm wide was used. A plunger-type wave generator was equipped at one end of the flume, and a mortar-made uniform slope of 1/20 was installed at the other end. In this experiment, a tray (60 cm long and 2 cm deep) was fixed on the slope after removal of a part of the bottom. The tray was always exposed to the action of broken waves with heights ranging from 1.8 to 3.2 cm and periods from 0.8 to 2.4 s. Five kinds of well sorted sediment with approximately the same specific gravity (about 2.6) but different diameters (0.23, 0.41, 0.79, 1.3, and 2.9 mm) were used. The amount of sediment tested was 1500 g for each compartment. The surf zone data available were incorporated to form a sound base for establishing a transport rate formula which is applicable to the whole range of the nearshore zone.

The data were analyzed with the Ursell number U_r representing the skewness of water particle velocity profile and the Hallermeier (1982) parameter Φ indicating the intensity of sediment movement, where

$$U_r = HL^2/d^3 \quad \text{and} \quad \Phi = (a_0\omega)^2/\gamma' gD$$

in which L is the wave length, a_0 is the near-bottom orbital diameter, ω is the wave angular frequency of waves, D is the grain size of the sediment, and γ' is the specific gravity of immersed sediment.

Figure 1 is a plot of net sediment transport directions on the U_r – Φ plane, showing that

(1) net sediment transport takes place if $U_r > 230$,
(2) onshore transport occurs if $7000/U_r < \Phi < 0.13\,U_r$,
and (3) offshore transport occurs if $\Phi > 0.13\,U_r$.

A quantitative examination of the data plotted in the figure indicated that the normalized sediment transport rate Q/wD can be expressed as a function of Φ for a fixed U_r, where Q is the volume (with void) rate of net onshore sediment transport per unit shoreline length, and w is the fall velocity of the sediment. In order to determine the functional form, the values of Q/wD were plotted against Φ for each range of U_r values, as shown in Fig. 2. Although the critical parameter value for net sediment transport is given by $\Phi_c = 7000/U_r$, data analysis on a quantitative basis suggests that an approximation of $\Phi_c = 0$ is reasonable.

Thus, the following functional form was assumed:

$$\frac{Q}{wD} = -A\,\Phi(\Phi - 0.13U_r) \tag{5}$$

where A is a function of U_r. The curves were drawn in Fig. 2 as a result of the best fit of Eq. (5) to the data. In spite of considerable data scatter, it is observed that general trends can be described by

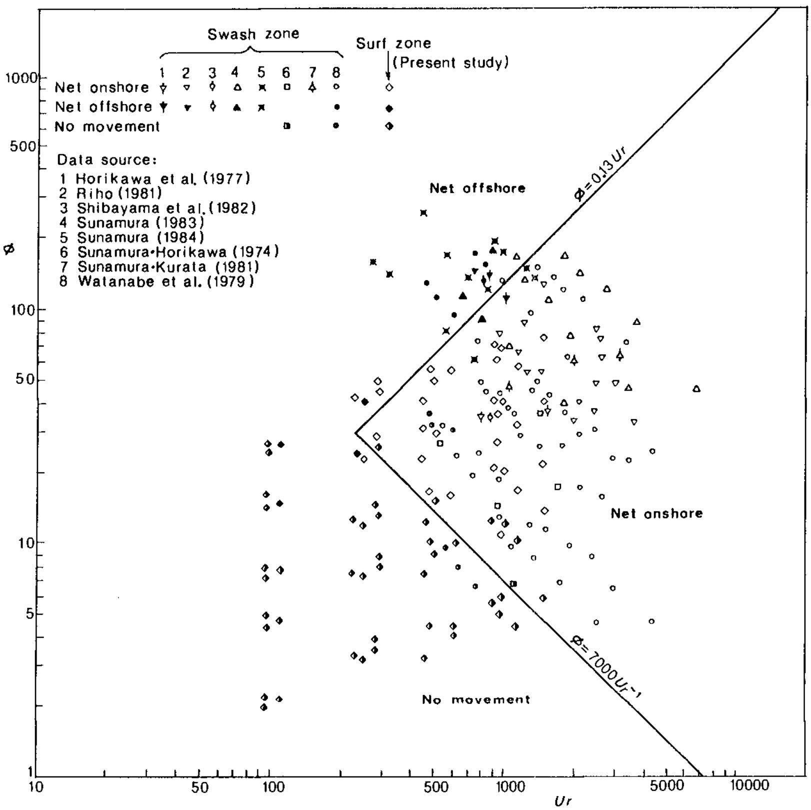

Fig. 1 Demarcation of net sediment transport directions.

this equation. A further plot showed that $A \sim U_r^{0.2}$, so that the following transport rate formula yields:

$$\frac{Q}{wD} = -BU_r^{0.2}\Phi(\Phi - 0.13U_r) \tag{6}$$

where B is a constant of the order 10^{-7} for laboratory tests of ordinary scale, and Q vanishes when $U_r < 230$.

Another set of data was obtained through prototype-scale experiments at the Central Research Institute of Electric Power Industry, Japan, and an investigation on these data indicated that B takes a value of the order 10^{-5} (Sunamura, 1984). As to this scale effect, however, a contradictive conclusion is derived from applications of the above formula as will be shown in Section 5. More studies are needed to fix the value of the coefficient.

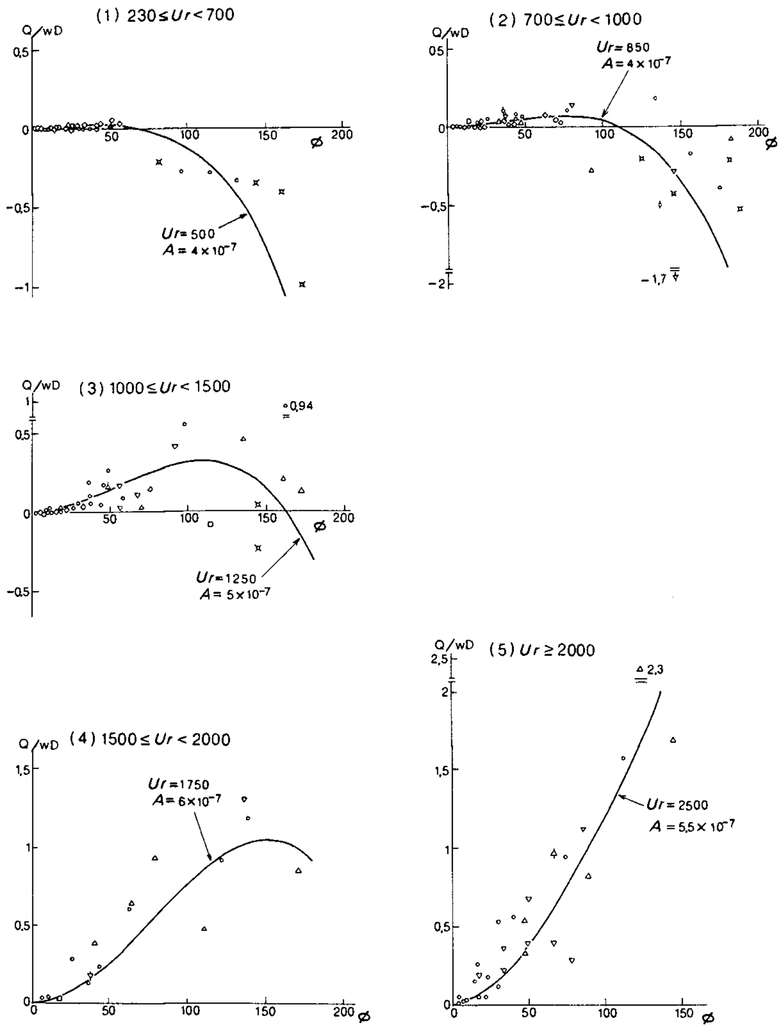

Fig. 2 Relationship between the normalized sediment transport rate Q/wD and the Hallermeier parameter Φ . (See the legend in Fig. 1 for symbols)

4. MODELING OF BEACH PROFILE CHANGES

The formula (6) gives the rate of net sediment transport as a function of local wave height and water depth, including no factor to represent the effect of bottom slope. As a consequence, a model simply based on the above formula may allow the generation of unrealistic local irregularities in the bottom topography. It is also impossible for the model to describe the reduction of net sediment transport which is normally observed as the beach profile approaches to an equilibrium slope.

On the basis of the above discussion, a term proportional to the excess bottom slope is introduced to give the effective sediment transport rate Q':

$$Q' = Q \mp \left(\left| \frac{\partial z}{\partial x} \right| - \beta_* \right) Q_* \tag{7}$$

where z is the bottom surface level and the modification is performed only when the absolute bottom slope exceeds the critical slope β_*. The scale of the modification Q_* is determined empirically as well as β_*. In the above expression, the inverse sign to that of $\partial z/\partial x$ is to be selected. Similar expression was used by Watanabe (1982) in his three-dimensional model.

Now, the continuity equation for bed material is written as follows:

$$\frac{\partial z}{\partial t} + \frac{\partial Q'}{\partial x} = 0 \tag{8}$$

where t is the time.

Let the values of the wave height and the water and bottom surface levels be defined at computation points $x = i\Delta x$ $(i = 0, 1, 2, \cdots)$ except those of the sediment transport rate which are defined at intermediate points $x = (i + 1/2)\Delta x$. Then, the rise of bottom surface Δz_i during the time interval Δt at the i-th point is given as

$$\Delta z_i = -(Q'_{i+1/2} - Q'_{i-1/2})\Delta t/\Delta x \tag{9}$$

in which the values of variables at the intermediate points required for the calculation of Q' are obtained through interpolation from those at neighboring definition points.

Simulation of the beach profile change is achieved by repetitive computations of the wave height, sediment transport rate and bottom surface level. It is recommended to adjust the time interval Δt at each time step of computation so that the resultant maximum change in the bottom surface level may not exceed a given limit. In order to save the computer execution time, variation of the wave height is calculated only when effective changes appeared in the beach profile.

5. EXAMPLE COMPUTATIONS

First, the result of a movable bed experiment of ordinary-scale is used for the examination of the numerical model. The bed material was well sorted sand with the grain size of 0.18 mm and the specific gravity of 2.7. The fall velocity of the material is estimated from Ruby's formula at 2.4 cm/s for the temperature of 15°C. A uniform slope of 1/10 was installed in a wave flume 17 m long, 60 cm high, and 40 cm wide. The bed was fixed and horizontal in the offshore range, where the water depth was 35 cm.

The slope was exposed to the continuous action of regular waves for 2 hours, and the profiles were measured several times after switching the wave generator off. A touch sensor was used for the measurement of the bottom level at every 5 cm along a longitudinal line. A representative profile was obtained through averaging profiles along 5 measuring lines at maximum, since the bottom topography was not necessarily uniform over the flume width. A typical bar was formed under the incident wave condition of 0.8 s in period and 6.7 cm in height.

Figures 3 show calculated wave height variations before and after the bar formation in comparison with experimental data. Calculated variations of the mean surface elevation are also shown by broken lines in the figures. The spacing of computation points Δx was fixed at 5 cm over the entire range of computation. A notable difference between the calculated and measured wave heights is found at their peaks near the breaking point. This is rather reasonable because the present model simulates the effective wave height which is proportional to the square root of wave energy density. Owing to the shoaling effect, a wave crest becomes steeper as it approaches to the breaking point, and a rapid increase in the apparent wave height is observed when it breaks.

Partial reflection of waves at the front slope of the bar causes a considerable undulation of wave height in the offshore range, as shown in the lower figure. A corresponding undulation also appears in the beach profile. Note that the wave reflection is not taken into account here in the computation. A more realistic results can be obtained through numerical integration of the decomposed mild slope equation with a dissipation term (Nishimura et al., 1983), although much more computational labor is required.

Figure 4 shows the beach profiles observed in the flume, whereas the results of numerical modeling is shown in Fig. 5. The profiles in Fig. 4 describe the very early stage of the observed process, involving already the major part of the profile changes. In the numerical computation, the parameter values such as $\beta_* = 0.1$ and $Q_* = 10^{-5}$ m^3/s were used, and the time interval Δt was adjusted in the range from 60 to 150 s. In spite of the comment in Section 3, the coefficient B was given the value of 10^{-5} here for the best fit to the measured profiles. The generation and development of a bar are well simulated by the numerical model, while the location of the bar is not correctly estimated.

As shown in Fig. 6, the rapid changes in the wave height and water depth result in the complicated variations of U_r and Φ values. The corresponding sediment transport rate is denoted by the broken line in Fig. 7. The solid line in the same figure shows the rate deduced from the observed profile changes. The peak of the former appears at the breaking point, whereas the peak of the latter is located on the back slope of the bar. In the numerical model, the predominant flushing effect appearing at the bar crest causes offshore shift of the bar and, consequently, that of the breaking point. Thus, the continuous and rather rapid move of the bar takes place. Such interactive deformations of waves and beach profile are often observed in a flume and in a field as well, although the speed of bar move is much lower.

The above-discussed defect of the model implies an inadequateness of the basic assumption that the rate of net sediment transport can be evaluated solely from local wave and topographic conditions. In fact,

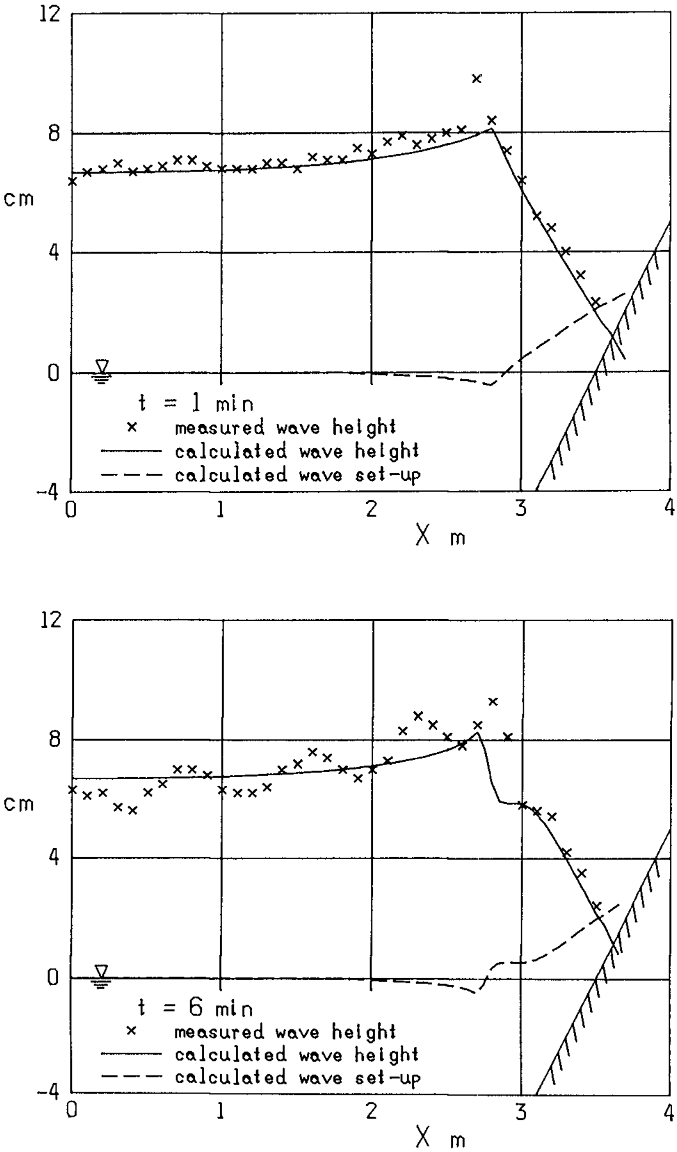

Fig. 3 Variation of the wave height and wave setup.

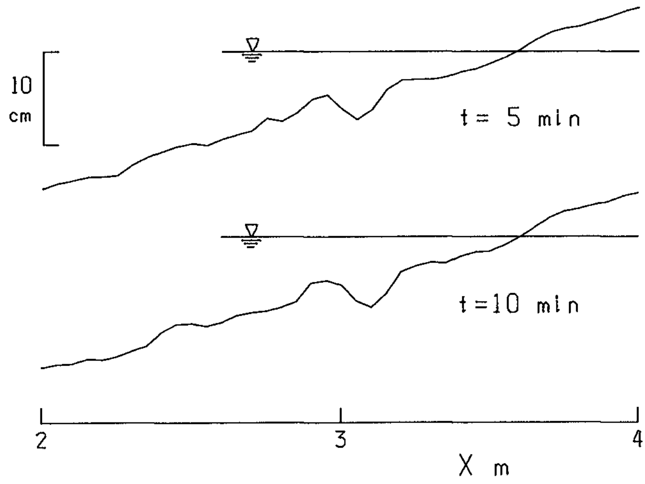

Fig. 4 Beach profiles observed in an ordinary-scale flume.

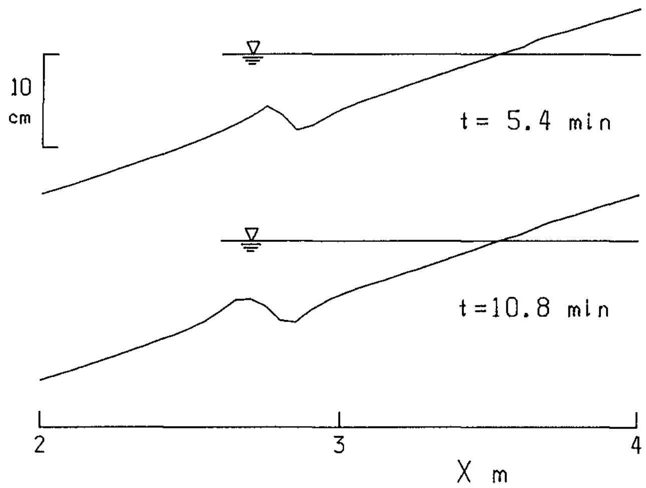

Fig. 5 Calculated beach profiles.

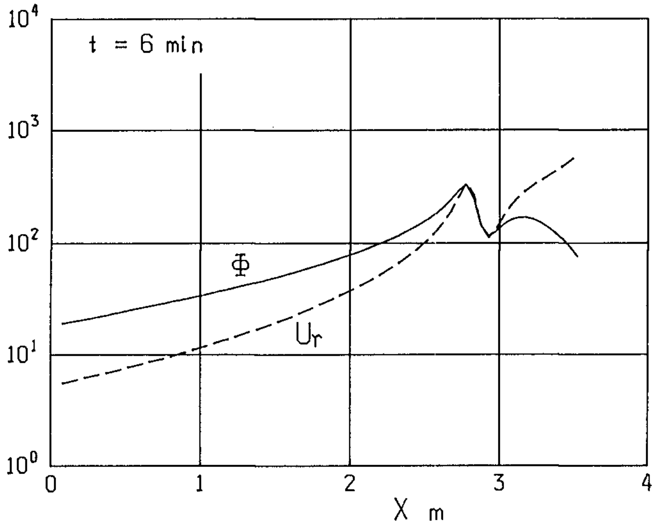

Fig. 6 Variations of the Ursell number U_r and the Hallelmeier parameter Φ.

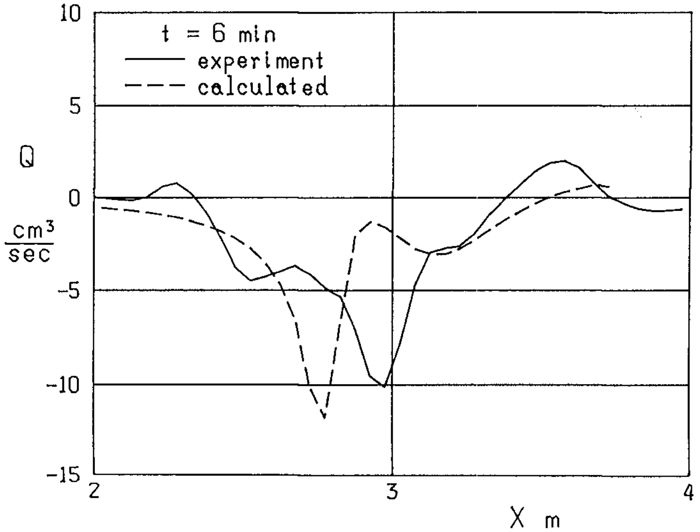

Fig. 7 Variation of the sediment transport rate.

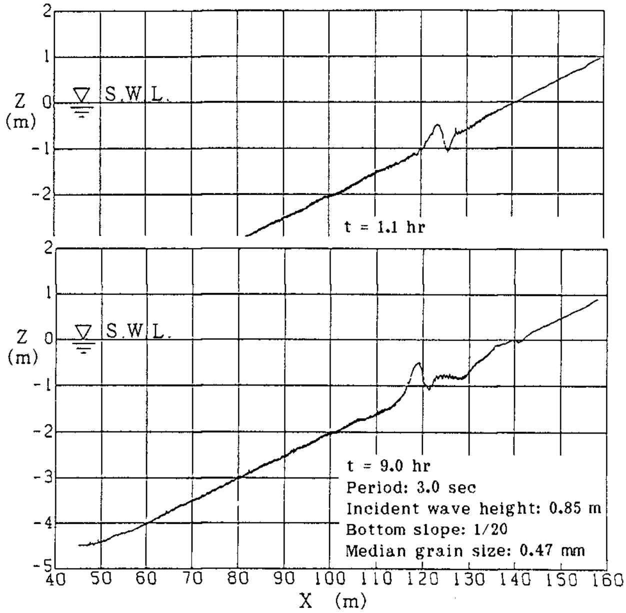

Fig. 8 Beach profiles observed in a prototype-scale flume.

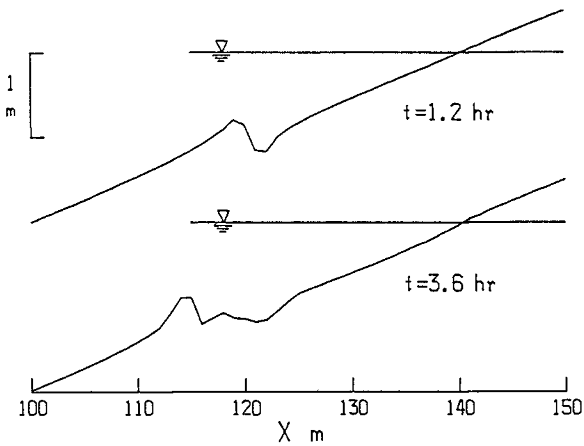

Fig. 9 Calculated beach profiles.

the intense near-bottom flows induced by plunging waves largely contribute to the bar and trough formation.

Figure 8 presents another example of beach transformation observed in the prototype-scale wave flume by Shimizu et al. (1985); experimental conditions are specified in the figure. The corresponding result of numerical hindcasting is shown in Fig. 9, which exhibits the similar tendencies to the preceding example. It is, however, interesting to point out that the numerical model well explain the generation of a secondary bar in the trough behind a main bar. In this example, the spacing Δx and the time interval Δt were expanded to 1 m and 10 - 30 min, and Q_* also proportionally to the maximum rate of net sediment transport. A note is that the value of coefficient B in the formula (6) was kept unchanged at 10^{-5} . It is thus concluded through these applications that the significant scale effect does not appear on this coefficient.

ACKNOWLEDGEMENTS

The authors are grateful to the Central Research Institute of Electric Power Industry, Japan, who kindly offered the experimental data for this study. The study was financially supported by the Science Research Fund of the Ministry of Education, Science and Culture, Japan, and also by the Project Research Fund of the University of Tsukuba.

REFERENCES

Goda, Y. (1970): A synthesis of breaker indices, Proc. Japan Soc. Civil Engrs., No.180, pp.39-49.

Hallermeier, R. J. (1982): Oscillatory bedload transport: Data review and simple formulation, Continental Shelf Res., Vol.1, pp.159-190.

Izumiya, T. and Horikawa, K. (1984): Wave energy equation applicable in and outside the surf zone, Coastal Eng. in Japan, Vol.27, pp.119-137.

Mizuguchi, M. and Mori, M. (1981): Modeling of two-dimensional beach transformation due to waves, Coastal Eng. in Japan, Vol.24, pp.155-170.

Nishimura, H. (1982): Numerical simulation of nearshore circulations, Proc. 29th Japan. Conf. on Coastal Eng., pp.333-337. (in Japanese)

Nishimura, H., Maruyama, K. and Hiraguchi, H. (1983): Wave field analysis by Finite Difference method, Proc. 30th Japan. Conf. on Coastal Eng., pp.123-127. (in Japanese)

Shibayama, T. (1984): Sediment Transport Mechanism and Two-Dimensional Beach Transformation Due to Waves, Doctoral Diss., Univ. Tokyo, 159p.

Shimizu, T., Saito, S., Maruyama, K., Hasegawa, H. and Kajima, R. (1985): Modeling of Onshore-Offshore Sand Transport Rate Distribution Based on the Large Wave Flume Experiment, Central Res. Inst. of Electric Power Industry, Civil Eng. Lab. Rep. No. 385050, 60p. (in Japanese)

Sunamura, T. (1982): Laboratory study of on/offshore sediment transport rate in shallow water region, Proc. 29th Japan. Conf. on Coastal Eng., pp.239-243. (in Japanese)

Sunamura, T. (1984): Prediction of on/offshore sediment transport rate in the surf zone including swash zone,Proc.31st Japan. Conf. on Coastal Eng., pp.316-320. (in Japanese)

Watanabe, A. (1982): Numerical models of nearshore currents and beach deformation, Coastal Eng. in Japan, Vol.27, pp.147-161.